

D15-2006-23

V. M. Bystritsky¹, Vit. M. Bystritskii², T. L. Enik¹,
M. Filipowicz³, V. V. Gerasimov¹, V. M. Grebenyuk¹,
A. P. Kobzev¹, R. V. Kublikov¹, V. V. Nesvizhevskii⁴,
S. S. Parzhitskii¹, V. N. Pavlov¹, N. P. Popov⁵,
A. V. Salamatin¹, V. N. Shvetsov¹, V. M. Slepnev¹,
A. V. Strelkov¹, J. Wozniak⁵, N. I. Zamyatin¹

EXPERIMENTAL RESEARCH OF THE RADIATIVE
CAPTURE OF THERMAL NEUTRONS IN ^3He

¹ Joint Institute for Nuclear Research, Dubna, Russia

² Department of Physics and Astronomy, University of California,
Irvine, USA

³ Faculty of Fuels and Energy, AGH University of Science and Technology,
Cracow, Poland

⁴ Institute Laue–Langevin, Grenoble, France

⁵ Faculty of Physics and Applied Computer Science, AGH University
of Science and Technology, Cracow, Poland

Быстрицкий В. М. и др.

D15-2006-23

Экспериментальное исследование процесса радиационного захвата тепловых нейтронов в ${}^3\text{He}$

Представлен проект эксперимента по измерению сечений радиационного захвата тепловых нейтронов ядрами ${}^3\text{He}$ с образованием одного и двух γ -квантов ($n_{\text{th}} + {}^3\text{He} \rightarrow \alpha + \gamma(2\gamma)$). Интерес к изучению данных процессов продиктован следующими обстоятельствами: возможностью получения информации о параметрах нуклонного ($N-N$)-потенциала и о структуре обменных мезонных токов; возможностью проверки модели механизма захвата нуклона ядром ${}^3\text{He}$ в низкоэнергетической области; необходимостью разрешения ряда вопросов, существующих в астрофизике. Выполнение эксперимента планируется осуществить на пучке PF1B реактора ILL (Гренобль). Мишень представляет собой полый цилиндр из чистого алюминия ($\varnothing 140 \times 80$ мм), заполняемый ${}^3\text{He}$ и ${}^4\text{He}$ (фоновый эксперимент) при давлении 2 атм. Регистрация γ -квантов осуществляется четырьмя детекторами на основе кристаллов BGO ($\varnothing 100 \times 70$ мм). Согласно расчетам, выполнение эксперимента позволит за 400–500 ч работы на пучке PF1B впервые измерить сечения указанных реакций с точностью 2–4% (одноквантовый процесс) и 7–10% (двухквантовый), что вполне отвечает целям проекта.

Работа выполнена в Объединенном институте ядерных исследований.

Сообщение Объединенного института ядерных исследований. Дубна, 2006

Bystritsky V. M. et al.

D15-2006-23

Experimental Research of the Radiative Capture of Thermal Neutrons in ${}^3\text{He}$

A project of an experiment on measurement of the cross sections of radiative thermal neutron capture by ${}^3\text{He}$ nuclei with production of one and two γ -quanta ($n_{\text{th}} + {}^3\text{He} \rightarrow \alpha + \gamma(2\gamma)$) is presented. The interest in studying the processes is dictated by the following factors: a possibility of obtaining information on parameters of the nucleon $N-N$ potential and structure of exchange meson currents; a possibility of verifying the model of the mechanism for nucleon capture by the nucleus ${}^3\text{He}$ in the low-energy region; necessity to solve some questions existing in astrophysics. The experiment is planned to be carried out on the PF1B beam of ILL reactor (Grenoble). The target is a hollow cylinder of pure aluminium ($\varnothing 140 \times 80$ mm) filled with ${}^3\text{He}$ and ${}^4\text{He}$ (background experiment) at the pressure 2 atm. Registration of the γ -quanta is carried out by four BGO crystal ($\varnothing 100 \times 70$ mm) detectors. According to the calculations the experiment, with 400–500 h of the PF1B beam running time, will allow cross sections for the above reactions to be measured for the first time with an accuracy of 2–4 % (one-quantum process) and 7–10 % (two-quantum process), which quite meets the purposes of the project.

The investigation has been performed at the Joint Institute for Nuclear Research.

Communication of the Joint Institute for Nuclear Research. Dubna, 2006

1. INTRODUCTION

The study of the processes occurring in few-body systems in the region of ultralow energy (\sim keV) is rather important and is connected with a possibility of describing a complicated system on the basis of the microscopic approach within the framework of modern nucleon–nucleon interaction concepts. However, the experimental study of reactions of proton interaction with light nuclei in the specified energy region is rather problematic. On the one hand, this is because the nuclear reactions cross section in the given energy region is small and, on the other hand, because the intensity of the charged particle beam produced by classical accelerators is low. Nevertheless, the information on characteristics of the given processes can be obtained at a certain level of accuracy from experimental studies of mirror reactions on light nuclei induced by neutrons.

Thus, comparison of the cross sections for the reactions of interest induced by protons and neutrons, lengths and phases of scattering (calculated within the same microscopic approach), and also their comparison with results of the experiments conducted on slow neutron beams will allow obtaining the information on potential (N – N) interactions and checking correctness of the algorithm of calculation of characteristics of mirror reactions.

In view of the aforesaid, the reactions of radiative capture of thermal neutrons by ${}^3\text{He}$ nuclei with production of one and two γ quanta: ${}^3\text{He}(n_{\text{th}}, \gamma){}^4\text{He}$ and ${}^3\text{He}(n_{\text{th}}, 2\gamma){}^4\text{He}$ deserve investigation.

Interest in these processes is dictated by a number of factors:

- 1) A possibility of obtaining information on the structure of the nucleon–nucleon (N – N) potential.
- 2) A possibility of studying the structure of the exchange meson currents whose contribution in the astrophysical energy region is essential [1].
- 3) Necessity of solving some questions existing in astrophysics.

Nuclear reactions induced by protons are essential for correct interpretation of entire picture of the processes proceeding in the Sun.

Therefore, the information on characteristics of these processes and in particular on the ${}^3\text{He}(p, e^+, \nu_e){}^4\text{He}$ reaction obtained in experiments on study of the mirror reaction ${}^3\text{He}(n_{\text{th}}, \gamma){}^4\text{He}$ will allow correct estimation of the intensity and

energy spectra of the solar neutrinos from the pp cycle like pp ($p+p \rightarrow d+e^++\nu_e$) and ppe ($p+p+e^+ \rightarrow d+e^++\nu_e$).

In view of possible oscillations between pp , ppe , hep , ${}^7\text{Be}$, ${}^{13}\text{N}$, and ${}^{15}\text{O}$ neutrinos, this will allow one to check applicability of the standard model to the description of the full set of processes taking place in the Sun [2–6]. The solar neutrino flux generated in the ${}^3\text{He}(p, e^+, \nu_e){}^4\text{He}$ reaction can be detected by a new generation of detectors characterized by a high energy resolution (due to neutrino–electron scattering or neutrino absorption). Since energy release in the ${}^3\text{He}(p, e^+, \nu_e){}^4\text{He}$ is rather high ($Q = 19.735$ MeV) and the neutrino detector has a rather high energy resolution, it becomes possible to detect a small fraction of the high-energy component of the solar neutrino flux which is essentially separated from the spectrum of the neutrinos produced in other reactions.

For their correct interpretation, the results of the solar neutrino flux measurement should be compared with the values calculated by the standard solar model. For lack of experimental data (at solar temperatures the mean kinetic energy of protons (~ 1 keV) is far below the Coulomb barrier of the ${}^3\text{He}$ nucleus and thus it is practically impossible to measure a very small cross section for capture of the proton by the ${}^3\text{He}$ nucleus), this model is based upon the calculated values of the ${}^3\text{He}(p, e^+, \nu_e){}^4\text{He}$ reaction cross section. Calculation of the ${}^3\text{He}(p, e^+, \nu_e){}^4\text{He}$ reaction cross section is also a problem.

However, the existing unique theoretical relation between matrix elements of the weak process ${}^3\text{He}(p, e^+, \nu_e){}^4\text{He}$ and the process of radiative neutron capture by the ${}^3\text{He}$ nucleus (${}^3\text{He}(n_{\text{th}}, \gamma){}^4\text{He}$) in the region of astrophysical energies saves the situation [7–9].

This statement is based upon the following:

a) In both above processes at ultralow energies (1–10 keV) neutron and proton capture proceeds from the S state of the nucleons. Therefore, not only the wave function of the nucleus in the final state (ground state of ${}^4\text{He}$) but also initial states of the ${}^3\text{He}+p$ and ${}^3\text{He}+n$ systems are identical (except charge-dependent factors).

b) In the impulse approximation the nonrelativistic forms of the single-particle dipole magnetic M1 and Gamow–Teller (GT) operators are similar except for rotation in the isospin space.

Though recently the solar neutrino riddle connected with the deficit of high-energy «boric» and «berillium-7» neutrinos has been resolved at a certain level of confidence (oscillation between electronic, muon and tau-neutrino are found), independent experimental information on each process entering into branched chain of processes occurring in the Sun is desirable for clarifying the balance between the intensities of three types of solar neutrinos.

4) A possibility of checking the model of the mechanism of nucleon capture by the ${}^3\text{He}$ nucleus in the low-energy region (S wave). In the standard model the dominating components of the wave functions describing the state of the

system before and after nucleon capture are symmetrical in orbital permutations and single-particle M1 or GT transitions may proceed through small components of low-orbit symmetry in both cases.

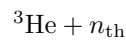
5) Knowledge of the cross section for the two-quantum process and the ratio of the $({}^3\text{He}(n_{\text{th}}, 2\gamma){}^4\text{He})$ and $({}^3\text{He}(n_{\text{th}}, \gamma){}^4\text{He})$ reaction cross sections will allow information on the structure of nuclear states participating in the above reactions, which is very important for adequate comparison of theory and experiment [10].

By now a number of experiments on measurement of cross sections of radiative neutron capture by nuclei ${}^3\text{He}$ have been carried out:

$$\begin{aligned}
\sigma(n_{\text{th}}, \gamma) &< 100 \mu\text{b} [11] (1960) - (\text{ILL, Grenoble}) \\
\sigma(n_{\text{th}}, \gamma) &= 60 \pm 30 \mu\text{b} [12] (1973) - (\text{ANL, USA}) \\
&= 60 \pm 12 \mu\text{b} [13] (1979) - (\text{ILL, Grenoble}) \\
&= 27 \pm 9 \mu\text{b} [14] (1979) - (\text{IBR-30, Dubna}) \\
&= 54 \pm 6 \mu\text{b} [15] (1979) - (\text{ILL, Grenoble}) \\
&= 55 \pm 3 \mu\text{b} [16] (1991) - (\text{Petten, Netherlands}) \\
\sigma(n_{\text{th}}, 2\gamma) &= 17 \pm 5 \mu\text{b} [13] (1979) - (\text{ILL, Grenoble}).
\end{aligned}$$

Recently interest in the studies of two-quantum radiative capture of thermal neutrons by the simplest nuclei has increased. In view of a possibility of testing quantum chromodynamics in neutron investigations numerous model calculations with various fine corrections were carried out. Now there is a great (more than an order of magnitude) discrepancy between the calculated value cross section of the reaction ${}^3\text{He}(n_{\text{th}}, 2\gamma){}^4\text{He}$ $\sigma_{\gamma\gamma}({}^3\text{He})$ [17, 18] and its sole experimental estimate [13]. The $\sigma_{\gamma\gamma}$ (th) measurement accuracy is $\sim 35\%$.

The goal of this project is to study the radiative capture of thermal neutrons by ${}^3\text{He}$ nuclei with production of one and two γ quanta



It is necessary to note that realization of this project will make it possible to clear out the nature of the existing discrepancy between the experimental and calculated values of the cross section for two-quantum radiative capture of thermal neutrons by nuclei ${}^3\text{He}$.

2. FORMULATION OF THE EXPERIMENT

Experiments on measurement of cross sections for reactions (1a) and (1b) face some difficulties, the main of which are the following:

- a) a small value of the cross sections for the processes of interest;
- b) presence of a competing channel (${}^3\text{He}(n_{\text{th}}, p)t$ reaction) with the intensity 10^8 and $4 \cdot 10^8$ times as high as the intensity of processes (1a) and (1b), respectively;
- c) a rather low detection efficiency for hard γ radiation (10–20 MeV) featured by traditional NaI(Tl)-based γ detectors;
- d) a high background level as compared with the process of interest.

Considering the importance of the task set, some changes are proposed for the experiment in comparison with the previous measurements [11–16] in order to measure the cross sections for reactions (1a) and (1b) with a high precision.

These changes are:

1) An arrangement of the experimental installation on the PF1B high-intensity beam of thermal neutrons of the ILL reactor (Grenoble, France).

2) Replacement of γ -quantum detectors based on NaI(Tl) crystals by detectors based on BGO crystals with a higher hard γ -quantum detection efficiency ($E_\gamma = 10\text{--}20$ MeV) on the one hand, and with an essentially smaller sensitivity to scattered neutron radiation on the other hand.

3) Precise determination of the absolute γ -quantum detection efficiency of the experimental setup by carrying out additional measurements with use of the tagget quantum flux from the reactions $p(t, \alpha)\gamma$ ($Q \approx 19.8$ MeV) and ${}^7\text{Li}(p, 2\alpha)\gamma$ ($Q \approx 17.3$ MeV) at the Van de Graaff accelerator and also with use of a set of standard radioactive sources.

4) Simultaneous use of the activation and time-of-flight techniques for measuring the surface density and energy distribution of incident neutrons.

5) A larger number of γ detectors, which, in turn, will allow measurement of not only the probability ratio of reactions (1a) and (1b) but also absolute values of their cross sections.

6) Optimization of the passive shielding of the γ detectors to suppress the background intensity to the level required by the project.

In the opinion of the authors of the project, realization of items 1)–6) will allow a significant increase in the accuracy of measurement of cross section for processes (1a) and (1b).

2.1. Experimental Setup. Figure 1 schematically shows the experimental setup mounted on the PF1B thermal neutron beam. The experimental setup comprises a collimator, a gaseous helium target, γ detectors with combined Pb, ${}^6\text{LiF}$ and polyethylene shielding. The neutron flux is formed by the collimator consisting of two ${}^6\text{LiF}$ plates (each ~ 10 mm thick with a 120×60 mm aperture for a beam of thermal neutrons) and a hollow polyethylene cylinder 200 mm

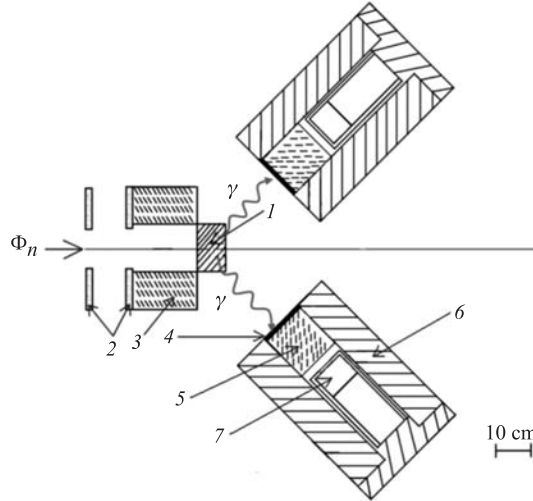


Fig. 1. Experimental setup: 1 — helium target; 2, 3 — collimator consisting of ${}^6\text{LiF}$ plates and hollow polyethylene cylinder; 4, 5 and 6 — combined ${}^6\text{LiF}$, polyethylene and Pb shielding of the detectors; 7 — four BGO crystal γ detectors

long with walls 120 mm thick. The flux of thermal neutrons with an average energy $4.0 \cdot 10^{-3}$ eV and surface density $\sim 3 \cdot 10^9$ n/cm 2 ·s hits the target, which is an Al cylinder ($\varnothing 140 \times 80$ mm) filled with pure ${}^3\text{He}$ at a pressure of 2 at. The side wall, the entrance window, and the exit window are 0.5, 0.1, and 0.1 mm thick, respectively. The volume of the target is 1230 cm 3 . To suppress the background flux in the γ detectors arising from neutron capture in target walls, the diameter of the target entrance window is larger than the diagonal of the neutron beam cross section (60×120 mm). Four BGO crystals ($\varnothing = 100$ mm, $h = 70$ mm) γ detectors are arranged in a circle around the axis of the neutron beam incident on the target (see Fig. 1). The angle between the axis of each γ detector and the direction of the neutron beam is 45° . The γ detectors are placed at a distance of 50 cm from the helium target center. The relative solid angle of the γ detector is $2.5 \cdot 10^{-3}$ and the detection efficiency for γ quanta with energy $E_\gamma \sim 20.6$ MeV (in total absorption peak) is $\sim 5\%$. Detection of the reaction (1b) channel is carried out by selection of coincidence of signals from any two γ detectors during the resolving time of 50 ns provided that their amplitudes correspond to the full absorption peak at the γ -quantum energy $E_{\text{thr}} < E_\gamma < 10.3 \text{ MeV} + 3 \sigma_E$ ($\sigma_E = 0.25$ MeV, $E_\gamma = 10.3$ MeV). For essential suppression of the relativistic components of background loading of the γ detectors they are surrounded by lead shielding. The background caused by the neutron radiation loading of the γ detectors by resulting from interaction of the beam of thermal

neutrons with a target, is suppressed by the combined absorber consisting of layers of ${}^6\text{LiF}$ (5 mm thick) and polyethylene (150 mm thick).

Prior to precise measurement of cross sections for radiative capture of thermal neutrons with production of one γ quantum, σ_γ (process (1a)), and two γ quanta, $\sigma_{\gamma\gamma}$ (process (1b)), a few additional experiments should be carried out for

1) measuring the detection efficiency of the experimental setup for γ quanta produced in reactions (1a) and (1b);

2) choosing the passive shielding of γ detectors that is optimal in terms of the background level;

3) measuring the energy and space distributions of neutrons in the PF1B flux (from the ILL reactor) by the activation and time-of-flight techniques.

2.2. Measurement of the γ -Quantum Detection Efficiency. Determination of the γ -quantum detection efficiency of the experimental setup in the study of reactions (1a) and (1b) implies studies of γ -detector responses in a wide γ -quantum energy range from 1 to 22 MeV with the use of standard γ -quantum sources (${}^{137}\text{Cs}$, ${}^{60}\text{Co}$, ${}^{88}\text{Y}$, ${}^{228}\text{Th}$, Po–Be) and reactions on light nuclei $t(p, \gamma)\alpha$ yielding γ quanta of energies $E_\gamma = E_p - E_\alpha + 19.8$ MeV (E_p and E_α are the laboratory energies of the proton and the α particles) and ${}^7\text{Li}(p, \gamma){}^8\text{Be}$ ($E_\gamma = E_p - E_{\text{Be}} + 17.3$ MeV).

Note that in case of the reaction $t(p, \gamma)\alpha$ a beam of «tagged» γ quanta is formed by simultaneous detection of the γ quantum and the α particle produced in this reaction (localization of the α -particle trajectory uniquely defines the direction of the emission of the γ quantum). For essential suppression of a quite intensive soft component of the background loading of the γ detectors, arising from the work on a beam of thermal neutrons the energy threshold in the spectrometer channel of γ -quantum registration should not be lower than 3 MeV.

Figure 2 shows the experimental layout for measurement of the detection efficiency of the «tagged» γ quanta from the $t(p, \gamma)\alpha$ reaction.

The quantum detection efficiency of the setup is defined as $\varepsilon_\gamma = N_{\alpha\gamma}/N_\alpha$, where $N_{\alpha\gamma}$ is the number of $\alpha\gamma$ coincidences corresponding to the number of α particles N_α registered by the α detector.

Thus, the technique of «tagged» γ quanta allows the detection efficiency of the experimental setup for γ quanta from reaction (1a) to be measured with a high accuracy. A monoenergetic beam of «tagged» γ quanta with the required energy is planned to be produced of the Van de Graaff accelerator of the Joint Institute for Nuclear Research (Dubna). Determination of the γ -quantum detection efficiency should be carried out under the conditions identical to those of the experiment on measurement of cross sections of the radiative capture of thermal neutrons by ${}^3\text{He}$ nuclei.

As to reaction (1b), considering the continuous spectrum of γ -quantum energies in the region from 0 to 21 MeV, dependence of the detection efficiency for γ quanta from this reaction upon energy in the region 0–21 MeV should be

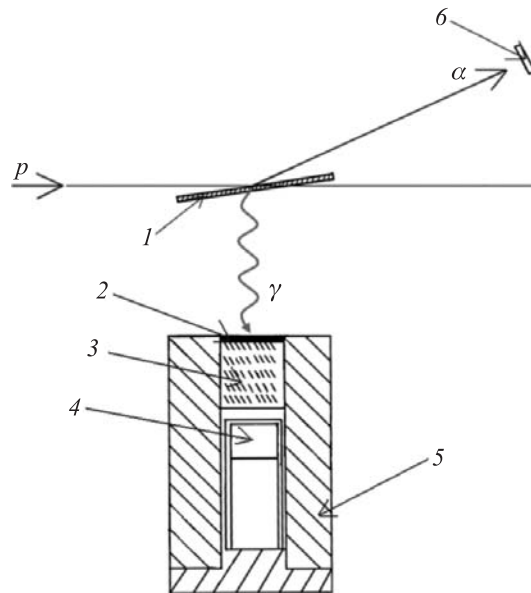


Fig. 2. Measurement of the detection efficiency of γ quanta with energy by the experimental setup. 1 — tritium target (TiT_2 , 2 μm thick); 2 — ${}^6\text{LiF}$ plate; 3 — polyethylene layer; 4 — γ detector; 5 — γ detector shielding of Pb; 6 — Si α detector; $I_p \approx 0.5\text{--}1 \mu\text{A}$ is the current of the protons incident on the target

known for correct measurement of cross section of the given process. Determination of the γ -quantum detection efficiency in the above energy range is based on comparison of shapes of the experimental amplitude distributions measured by the γ detectors and the distributions resulting from the Monte-Carlo simulation of interactions of γ quanta with the BGO crystal.

Thus, the γ -quantum detection efficiency is determined by calculation on condition that the experimental and simulated amplitude distributions of the events recorded by the γ detector coincide in shape. To optimize the design and composition of the shielding of the γ detectors against background radiation, it is planned to carry out measurements with these detectors at the IBR-2 reactor (JINR, Dubna). In addition, preliminary experiments at the reactor also include development of activation analysis and time-of-flight techniques for measurement of the energy and space distributions of thermal neutrons in a beam. The above, measurements at the IBR-2 reactor (JINR) will essentially reduce the time necessary for realization of the present project on the PF1B beam of the ILL reactor.

After all the above-mentioned work is accomplished in Dubna, the experimental set up is moved to the ILL reactor, where both the energy and space distributions of incident neutrons on the target of the PF1B beam are measured.

Below the procedures for measurement of the space and energy distributions of neutrons in the PF1B beam are described in more detail.

2.3. Measurement of the Neutron Spatial and Energy Distributions.

In the proposed scheme of the experiment the neutron flux incident on the target can be uniquely considered as plane parallel. This is proved by the entrance collimator design, the size of the helium target and its position relative to the flux, the amount of angular divergence of the neutron beam, and also the results of a lot of earlier experiments on measurement of the spatial distribution of neutrons in the PF1B beam carried out in ILL.

To measure cross sections σ_γ and $\sigma_{\gamma\gamma}$ for reactions (1a) and (1b), one should know with a high accuracy the energy distribution $\Phi_n(E)$ of neutrons in the flux incident on the ^3He -filled target.

Since the cross sections σ_γ and $\sigma_{\gamma\gamma}$ are the result of averaging over the energy spectrum of incident neutrons (with allowance for the Maxwellian velocity distribution of target atoms), the effective cross section $\sigma_\gamma(\text{th})$ at the point corresponding to the thermal neutron energy $E_{\text{th}} = 25.3$ meV [19] is used. The formula for determination of the effective reaction (1a) cross section $\sigma_\gamma(\text{th})$ has the form

$$\sigma_\gamma(\text{th}) = \frac{(N_\gamma/T)\sigma_t(\text{th}) \cdot \sqrt{\pi E_{\text{th}}/E_n}}{2\Phi_n S \cdot k\varepsilon_\gamma\Omega_\gamma \cdot 1 - e^{-n(\sigma_{\text{tot}})l}}, \quad (2)$$

where N_γ is the number of detected γ quanta from reaction (1a); l is the target thickness along the neutron flux; k is the number of γ detectors; ε_γ is the γ -quantum detection efficiency of the detector at full absorption peak; Ω_γ is the solid angle of the γ detector; $\sigma_t = \sigma_{pt} + \sigma_s + \sigma_\gamma + \sigma_{\gamma\gamma}$ is the total $n_{\text{th}}\ ^3\text{He}$ reaction cross section at the thermal point ($E_{\text{th}} = 25.3$ meV); $\langle\sigma_t\rangle$ is the total $n_{\text{th}}\ ^3\text{He}$ interaction cross section averaged over the energy spectrum of incident neutrons; S is the area of the incident neutron beam cross section; E_n is the neutron energy corresponding to the maximum of the Maxwellian distribution $\Phi_n(E)$; T is the measurement time. The second term in (2) is seen to take into account the shift of the Maxwellian distribution peak (E_n) relative to the peak corresponding to the thermal neutron energy (E_{th}).

The neutron energy distribution $\Phi_n(E)$ at the target site can be measured by various methods, for example, by the activation technique. This technique supposes the use of a set of m foils 3×3 cm² in area of total thickness such that neutron absorption coefficient of this stack of foils is less than 10%. Actually, two sets of the foils are supposed to be used, one placed in front of the entrance window of the target and the other behind its exit window. The methodological experiment allows correct account to be taken of the dynamics of the neutron flux passing through the ^3He -filled target. Measuring the induced activity in the k th foil A_k per target atom, which is related to the neutron energy distribution

function $\Phi_n(E)$ and the copper activation cross section $\sigma_k^{\text{Cu}}(E)$ by the formula [16]:

$$A_k = \int_0^{\infty} \Phi_n(E) \sigma_k^{\text{Cu}}(E) dE \quad (k = 1, \dots, m), \quad (3)$$

one can get the necessary information on the beam of neutrons.

The function $\Phi_n(E)$ is found by χ^2 comparison of the experimentally measured dependence of the induced activity A in the Cu foil upon the number of the foil and the analogous dependence calculated by the Monte-Carlo method and corresponding to a particular energy distribution of incident neutrons. Varying parameters of the function $\Phi_n(E)$ and using two sets of experimental values A_k corresponding to two stacks of Cu foils, one can get rather accurate information on the neutron energy distribution at the collimator exit. Note that errors in measurement of induced activities A_k , as follows from the simulation, are no larger than 1–2%.

Comparison of the activation analysis results and amplitude spectra of γ quanta registered by the γ detectors with indications of the neutron beam monitor will allow the parameters of the neutron flux and the experimental setup to be monitored and measured during the experiment. In addition, the neutron energy distribution of $\Phi_n(E)$ at the size of the target can also be measured by a mechanical monochromator.

2.4. Sources of Background. Since the cross sections for the processes of interest (reactions (1a) and (1b)) are extremely small, it becomes very important to study the nature of the background sources to get them considerably suppressed against the effect.

The background sources are: a) nuclear reactions with production of γ quanta and neutrons arising from interaction of the thermal neutron beam with the entrance window of the target and its side walls ($\text{Al}(n_{\text{th}}, n'\gamma)\text{Al}$); b) elastic scattering of thermal neutrons on ^3He nuclei with their subsequently registration by the γ detectors; c) (p, γ) and (t, γ) reactions arising from interaction of protons and tritons formed in the $^3\text{He}(n, p)t$ reaction with the target walls; d) delayed neutrons in the experimental hall; e) (n, γ) reactions on the structural materials of the experimental setup; f) chain of processes with subsequent registration of γ quanta by the BGO detectors: $^3\text{He}(n_{\text{th}}, p)t \rightarrow ^3\text{He}(t, d) ^4\text{He} \rightarrow ^3\text{He}(d, \gamma)^5\text{Li}$; g) chain of processes with subsequent registration of fast neutrons by the γ detectors: $^3\text{He}(n_{\text{th}}, p)t \rightarrow ^3\text{He}(t, pn) ^4\text{He}$; h) chain of processes with subsequent registration of hard γ quanta by the BGO detectors: $^3\text{He}(n_{\text{th}}, p)t \rightarrow ^3\text{He}(t, \gamma)^6\text{Li}$; i) the charged component of the cosmic radiation.

Below intensities of the above background sources are estimated in relation to the expected yield of reactions (1a) and (1b).

3. THE YIELD OF γ QUANTA FROM REACTIONS (1a) AND (1b)

3.1. One-Quantum Mode. The experimental yield Y_γ of γ quanta resulting from reaction (1a) can be written down as follows (the target volume specified by the size of the neutron flux collimator is $V = a \times b \times l$):

$$Y_\gamma = \varepsilon_\gamma \Omega_\gamma k \int_{x=0}^a \int_{y=0}^b \int_{z=0}^l \Phi_n(x, y, z) \langle \sigma_\gamma \rangle n dx dy dz, \quad (4)$$

where $\Phi_n(x, y, z)$ is the surface density of the thermal neutron flux on a perpendicular target area of 1 cm^2 at the point with the coordinates (x, y, z) ; $\langle \sigma_\gamma \rangle$ is the reaction (1a) cross section averaged over the energy spectrum of the neutrons incident on the target; n is the nuclear density of the target in cm^{-3} .

Considering attenuation of the neutron flux on its passage through the target in the Z direction, expression (4) takes the form:

$$Y_\gamma = k \varepsilon_\gamma \Omega_\gamma S \int_0^l \Phi_n(x, y, z) \langle \sigma_\gamma \rangle n dz = \Phi_0 S k \varepsilon_\gamma \Omega_\gamma (1 - e^{-n \langle \sigma_{\text{tot}} \rangle l}) \frac{\langle \sigma_\gamma \rangle}{\langle \sigma_{\text{tot}} \rangle}, \quad (5)$$

$$\Phi_n(x, y, z) = \Phi_0 e^{-n \langle \sigma_{\text{tot}} \rangle z}, \quad (6)$$

where $S = a \times b$ is the area of the beam incident on the target X - Y section, l is the target thickness in the Z direction, $\Phi_n(x, y, 0)$ is the surface density of the thermal neutron flux at the point $(x, y, 0)$.

In this case the cross section for one-quantum capture of thermal neutrons by ${}^3\text{He}$ nuclei is defined as

$$\langle \sigma_\gamma \rangle = \frac{N_\gamma \langle \sigma_{\text{tot}} \rangle}{\Phi_n S (1 - e^{-n \langle \sigma_{\text{tot}} \rangle L}) k \varepsilon_\gamma \Omega_\gamma T}, \quad (7)$$

where N_γ is the number of γ quanta with energy $E_\gamma = 20.6 \text{ MeV}$ detected within the time T . The real yield of γ quanta is described by a more complicated formula taking into account multiple elastic scattering of thermal neutrons on target walls and in ${}^3\text{He}$. The contribution from these processes is correctly calculated by the Monte-Carlo method.

Therefore, in (7) l is replaced by L , which is the total path of thermal neutrons (the path of the neutron in the target over a broken trajectory from the point where it hits the target to the point of its radiative capture with production of one or two γ quanta with allowance for elastic scattering of the neutrons from ${}^3\text{He}$ nuclei and rescattering on target walls) averaged over the real distribution of paths in the target.

3.2. Two-Quantum Mode. To measure the cross section $\sigma_{\gamma\gamma}$, events simultaneously detected by two γ detectors and meeting the criterion $E_{\gamma_1} + E_{\gamma_2} = B$ should be selected for analysis, where E_{γ_1} and E_{γ_2} are the energies of the γ quanta, B is the neutron binding energy in the ${}^4\text{He}$ nucleus. Relation between the cross sections for reactions (1a) and (1b) averaged over the energy spectrum of incident neutrons is described as follows [20]:

$$\langle\sigma_{\gamma\gamma}\rangle = \langle\sigma_{\gamma}\rangle \frac{N_{\gamma\gamma}}{N_{\gamma}} \frac{\varepsilon(B)}{m[\varepsilon_1(E_{\gamma_1})\varepsilon_2(B - E_{\gamma_1})] \Omega_2}, \quad (8)$$

where N_{γ} is the number of detected γ quanta from reaction (1a); $N_{\gamma\gamma}$ is the number of detected $\gamma\gamma$ coincidences in reaction (1b); ε_1 and ε_2 are the γ -quantum detection efficiencies of each of two γ detectors connected in coincidence, averaged over the continuous spectrum of γ radiation from two-quantum capture of thermal neutrons by ${}^3\text{He}$ nuclei. The yield of reaction (1b) with emission of two γ quanta on the assumption of a uniform surface density distribution of the incident neutron flux Φ_0 is

$$\begin{aligned} Y_{\gamma\gamma} &= S\varepsilon_{\gamma\gamma}mk\Omega_{\gamma}^2 \int_0^l \Phi_n(E)e^{-n\langle\sigma_{\text{tot}}\rangle z} \langle\sigma_{\gamma\gamma}\rangle ndz = \\ &= \Phi_0 S\varepsilon_{\gamma\gamma}mk\Omega_{\gamma}^2 (1 - e^{-n\langle\sigma_{\text{tot}}\rangle l}) \frac{\langle\sigma_{\gamma\gamma}\rangle}{\langle\sigma_{\text{tot}}\rangle}, \end{aligned} \quad (9)$$

where $\varepsilon_{\gamma\gamma} = \varepsilon_{\gamma_1}(E_{\gamma_1})\varepsilon_{\gamma_2}(20.6 - E_{\gamma_1}) + \varepsilon_{\gamma_2}(E_{\gamma_2})\varepsilon_{\gamma_1}(20.6 - E_{\gamma_2})$ is the intrinsic detection efficiency for coincidence of two quanta from (1b) (this value is averaged over possible kinematic combinations of energy distribution between two detected γ quanta), Ω_{γ} is the solid angle of the γ detector, k is the number of γ detectors, m is the number of possible pair combinations of γ detectors.

The effective reaction (1b) cross section averaged over the energy spectrum of neutrons interacting with the target is defined as

$$\langle\sigma_{\gamma\gamma}\rangle = \frac{N_{\gamma\gamma}\langle\sigma_{\text{tot}}\rangle}{\Phi_0 S(1 - e^{-n\langle\sigma_{\text{tot}}\rangle l})\varepsilon_{\gamma\gamma}km\Omega_{\gamma}^2 T}. \quad (10)$$

3.3. Evaluation of the Yields of Reactions (1a) and (1b). Table 1 lists estimates of the data taking time in the PF1B beam of thermal neutrons at the ILL reactor required for measurement of the cross sections $\langle\sigma_{\gamma}\rangle$ and $\langle\sigma_{\gamma\gamma}\rangle$ with the relative accuracy δ .

The following values were used to obtain the estimates:

$S = 72 \text{ cm}^2$, $\varepsilon_{\gamma} = 5 \cdot 10^{-2}$ (the intrinsic efficiency of registration of γ quanta from reaction (1a) at full absorption peak $E_{\gamma} - 3\sigma_E < E_{\gamma} < E_{\gamma} + 3\sigma_E$ $E_{\gamma} =$

Table 1. Time T of exposure of the setup on the ILL reactor beam PF1B for measurement of the reaction (1a) and (1b) cross sections with the given accuracy δ (%)

Accuracy δ , %	Reaction (n_{th}, γ)		Reaction ($n_{\text{th}}, 2\gamma$)	
	T_{exp} , h	Yield, N_γ	T_{exp} , h	Yield, $N_{\gamma\gamma}$
10	0.1	330	140	100
5	0.25	830	560	400
2	1.5	5000	3500	2500

20.6 MeV; $\sigma_E = 0.5$ MeV is the energy resolution of the γ detector for the line of 20.6 MeV), $\varepsilon_{\gamma\gamma}$ is the intrinsic efficiency of detection of two γ quanta from reaction (1b) in any pair from four γ detectors (connected in coincidence), $\varepsilon_{\gamma\gamma} = 6.4 \cdot 10^{-3}$ ($E_{\text{thr}} < E_\gamma < 10.3$ MeV + $3 \cdot \sigma_E$ ($E_\gamma = 10.3$ MeV, $\sigma_E = 0.25$ MeV), $\Omega_\gamma = 2.5 \cdot 10^{-3}$ is the solid angle of the γ detector, $\langle\sigma_\gamma\rangle = 50$ μb , $l = 8$ cm, $\langle\sigma_{\gamma\gamma}\rangle = 10$ μb , $\Phi_0 = 3 \cdot 10^9$ n/cm²·s, $\langle\sigma_t\rangle = 5300$ b, $n = 5.4 \cdot 10^{19}$ cm⁻³.

It is necessary to note that estimates of the background level caused by sources listed in Subsec. 2.4 are obtained with some criteria imposed on the events registered by the γ detectors. For example, only events falling within the γ -quantum energy region $E_\gamma - 3\sigma_E < E_\gamma < E_\gamma + 3\sigma_E$ ($E_\gamma = 20.6$ MeV; $\sigma_E = 0.5$ MeV is the energy resolution of γ detector on a line 20.6 MeV) are selected for studying reaction (1a) and events falling within the energy region $E_{\text{thr}} < E_\gamma < 10.3$ MeV + $3\sigma_E$ ($E_\gamma = 10.3$ MeV, $\sigma_E = 0.25$ MeV) are selected for studying reaction (1b). With these rigid event selection criteria, the imitation of processes (1a) and (1b) with the existing sources of the background is possible only within the data-acquisition equipment resolving time of 50 ns several background quantum are detected (by one γ detector in case of studying reaction (1a), or two γ detectors in case of studying reaction (1b)). The resulting signal amplitude should correspond to the criteria for selection of events by the energy lost by γ quanta in the BGO crystal.

Using the Monte-Carlo method we considered in detail background sources (a)–(h). The calculations showed that the total background in relation to the reaction yield does not exceed 40% for (1a) and 1% for (1b). As to the background caused by cosmic radiation its level was determined experimentally with use of the γ detector and the spectrometer path similar to those to be used in the planned experiment. Combined shielding of polyethylene, ⁶LiF and Pb layers corresponding to the conditions of the experiment on the ILL reactor beam was used for the γ detectors. The results of the measurements indicate that the background level in the relation to the reaction yield is 5% for reaction (1a) and negligibly small for reaction (1b).

Figures 3 and 4 show dependence of the σ_γ and $\sigma_{\gamma\gamma}$ measurement accuracy upon the data taking time.

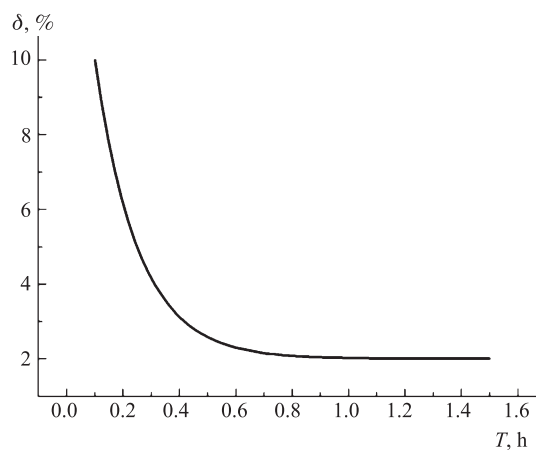


Fig. 3. The accuracy of measurement of the cross section $\langle\sigma_{\gamma}\rangle$ versus the data taking time

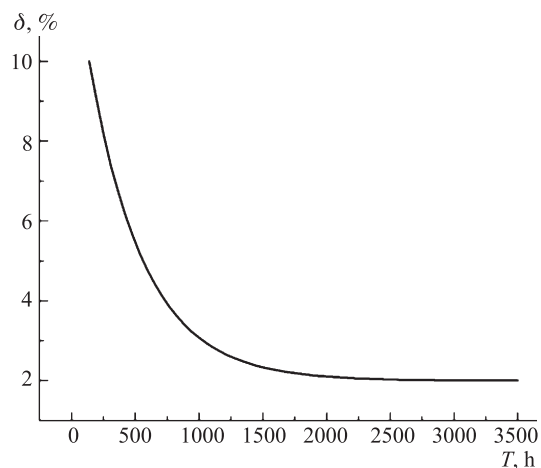


Fig. 4. The accuracy of measurement of the cross section $\langle\sigma_{\gamma\gamma}\rangle$ versus the data taking time

To test the calculated estimates of the background levels in studies of processes (1a) and (1b), and to get their more precise values, we plan to carry out a separate background experiment with a target filled with gaseous ^4He to a pressure of 2 at.

3.4. Background Experiment. In this experiment the same target as the experiment with pure ^3He is used.

Let us consider the relation between the calculated intensities of various background processes in case of filling target with ^3He and ^4He at a pressure

of 2 at. Partial contributions of the various background processes mentioned in Subsec. 2.4 (sources of background) are compared in Table 2.

Table 2. Comparison of the estimated intensities of various sources of background in the experiment with a target filled with ^3He and ^4He . The equality of the background levels in exposures with ^3He and ^4He is marked by the sign «+» in the corresponding columns; the combination of the signs «+» and «-» means excess of the background level in the exposure to which there corresponds the sign «+»

No	Background sources	^3He target, 2 at	^4He target, 2 at
1	Interaction of neutron beam with collimator	+	+
2	Interaction of neutron beam with target front wall	+	+
3	Interaction of neutron beam with target back wall (on passing through target)	-	+
4	Interaction of products of reaction $^3\text{He}(n,p)t$ with walls of target	+	-
5	Interaction of beam of neutrons scattered on gas (^3He , ^4He) with target walls	-	+
6	Neutron beam scattering on (^3He , ^4He) with subsequent registration of neutrons by γ detectors	-	+
7	Chain of processes with subsequent registration of γ quanta by the BGO detectors: $^3\text{He}(n_{\text{th}}, p)t \rightarrow ^3\text{He}(t, d)^4\text{He} \rightarrow ^3\text{He}(d, \gamma)^5\text{Li}$	+	-
8	Chain of processes with subsequent registration of fast neutrons by the γ detectors: $^3\text{He}(n_{\text{th}}, p)t \rightarrow ^3\text{He}(t, pn)^4\text{He}$	+	-
9	Chain of processes with subsequent registration of hard γ quanta by the BGO detectors: $^3\text{He}(n_{\text{th}}, p)t \rightarrow ^3\text{He}(t, \gamma)^6\text{Li}$	+	-

Comparison of calculated intensities of various sources of background by a method of Monte Carlo resulted in Table 2, testify that distinction in total levels of background in experiment with ^4He and ^3He does not exceed 15%:

$$\eta = (N_{\text{cal}}^{\text{backg}}(^4\text{He}) - N_{\text{cal}}^{\text{backg}}(^3\text{He})) / N_{\text{cal}}^{\text{backg}}(^3\text{He}) \approx 0.15, \quad (11)$$

where $N_{\text{cal}}^{\text{backg}}(^3\text{He})$, $N_{\text{cal}}^{\text{backg}}(^4\text{He})$ are the normalized calculated numbers of the registered background events in the experiment with ^3He and ^4He (simulating the event of registration of γ quanta from reaction (1a)); $\delta_\eta = 0.05$ is the relative error of the calculation of η . Considering accuracy of the calculation of η and the total background level ξ measured in the experiment with ^4He (according to the calculations this normalized value in relation to the yield of reaction (1a) in

the experiment with ${}^3\text{He}$ is $\approx 50\%$), it is possible to determine unambiguously the background level in the experiment with ${}^3\text{He}$ with its measurement error:

$$N^{\text{backg}}({}^3\text{He}) = \xi(1 - \eta), \quad (12)$$

$$\xi = N_{\text{meas}}^{\text{backg}}({}^4\text{He})\Phi_n({}^3\text{He})/\Phi_n({}^4\text{He}),$$

where $\Phi_n({}^3\text{He})$, $\Phi_n({}^4\text{He})$ are the full beam of thermal neutrons incident on the target in the experiments with ${}^3\text{He}$ and ${}^4\text{He}$, respectively.

According to the calculated estimates of ξ , η , and δ_η , an additional error of the measurement of the reaction (1a) cross section due to the proposed procedure of the background determination in the experiment with ${}^3\text{He}$ is $\approx 0.7\%$. As to measurement of the background level in case of the reaction (1b) study, the situation is more trivial. It is caused by the following circumstances. Firstly, the difference between the calculated (normalized) background levels in the study of reaction (1b) in exposures with ${}^3\text{He}$ and ${}^4\text{He}$ is negligibly small. Secondly, the absolute value of the background in the exposure with ${}^3\text{He}$ in relation to the yield of reaction (1b) (with the use of the selection criteria for registered events) indicated in the text of the project is extremely small ($\leq 1\%$). Thus, it follows that the background value measured in the experiment with ${}^4\text{He}$ and normalized to the exposure with ${}^3\text{He}$, defines to quite a high accuracy the background level in the experiment with ${}^3\text{He}$.

4. CONCLUSIONS

Having estimated yields of reactions (1a) and (1b) and having studied possible sources of the background and their influence on the accuracy of the measured cross sections of the reactions in question we may draw the following conclusions:

1) Implementation of this project on the PF1B beam of the ILL reactor will make possible to measure for the first time the cross section for process (1b) with statistical accuracy 7–10% and the absolute value of the cross section for process (1a) with accuracy of 2–4% for 400–500 h of the beam time.

2) The knowledge of the cross sections of the processes with the above accuracy will allow:

a) refining calculations of a chain of nuclear processes within the framework of the standard solar model;

b) obtaining information on the structure of the ground states of the ${}^3\text{He}$ and ${}^4\text{He}$ nuclei;

c) obtaining information on the nucleon–nucleon potential and the contribution of the exchange meson currents.

REFERENCES

1. *Towner I.S., Khanna F.C.* Intern. Conf. on Nuclear Physics with Electromagnetic Interactions. Mainz, 1979. V. 7. P. 12.
2. *Gerstein S.* http://baclanout.abitu.ru/ims/cfmsgm/j_i8amm/l_kbamm/p0edmm.html
3. *Bahcal J.* Neutrino Astrophysics. M., 1993.
4. <http://www.physics.upenn.edu/~www/neutrino/>
5. <http://www.maths.qmw.ac.uk/~lms/research/neutrino.html>
6. *Bahcal J.N., Pinsonneault M.H., Basu S.* Solar Models: Current Epoch and Time Dependence, Neutrinos, and Helioseismological Properties // *Astrophys. J.* 2001. V. 555. P. 990.
7. *Wertz C., Brennan J.G.* // *Phys. Rev.* 1967. V. 157. P. 759.
8. *Wertz C., Brennan J.G.* // *Phys. Rev. C.* 1973. V. 8. P. 1545.
9. *Tegner P.E., Bargholtz C.* // *Astrophys. J.* 1983. V. 272. P. 311.
10. *Acaishi Y. et al.* // *Progr. Theor. Phys.* 1974. V. 51. P. 134, 155.
11. *Galmann A., Kane J., Pixley R.* // *Bull. Am. Phys. Soc.* 1960. V. 5. P. 19.
12. *Bollinger L.M., Specht J.R., Thomas G.E.* // *Am. Phys. Soc.* 1973. V. 18. P. 591.
13. *Suffert M., Berthollet R.* // *Nucl. Phys. A.* 1979. V. 318. P. 54.
14. *Alfimenkov V.P. et al.* // *JETP Lett.* 1979. V. 29. P. 91.
15. *Wolfs F.L.H. et al.* // *Phys. Rev. Lett.* 1989. V. 63. P. 2721.
16. *Wervelman R. et al.* // *Nucl. Phys. A.* 1991. V. 526. P. 265.
17. *Blomqvist J., Ericson T.* // *Phys. Lett. B.* 1975. V. 57. P. 115.
18. *Cambi A. et al.* // *Nuovo Cimento A.* 1979. V. 47. P. 421.
19. *Westcott C.H.* // *J. Nucl. Energy.* 1955. V. 2. P. 59.
20. *Sharapov E.I.* // *Particles and Nuclei.* 1981. V. 12, No. 4. P. 962.

Received on February 16, 2006.

Корректор *Т. Е. Понько*

Подписано в печать 30.03.2006.

Формат 60 × 90/16. Бумага офсетная. Печать офсетная.

Усл. печ. л. 1,18. Уч.-изд. л. 1,67. Тираж 200 экз. Заказ № 55286.

Издательский отдел Объединенного института ядерных исследований
141980, г. Дубна, Московская обл., ул. Жолио-Кюри, 6.

E-mail: publish@pds.jinr.ru

www.jinr.ru/publish/